Liquid Crystals
Publication details, including instructions for authors and subscription information:
http://www.informaworld.com/smpp/title~content=t713926090

Synthesis and mesomorphic properties of some esters of trans-4-n-alkoxycinnamic and trans-4-n-alkoxy-alpha-methylcinnamic acids exhibiting ferroelectric and antiferroelectric phases

N. Kasthuraiah; B. K. Sadashiva; S. Krishnaprasad; Geetha G. Nair

To cite this Article Kasthuraiah, N. , Sadashiva, B. K. , Krishnaprasad, S. and Nair, Geetha G.(1998) 'Synthesis and mesomorphic properties of some esters of trans-4-n-alkoxycinnamic and trans-4-n-alkoxy-alpha-methylcinnamic acids exhibiting ferroelectric and antiferroelectric phases', Liquid Crystals, 24: 5, 639 — 645

To link to this Article: DOI: 10.1080/026782998206740

URL: http://dx.doi.org/10.1080/026782998206740

LIQUID CRYSTALS, 1998, VOL. 24, NO. 5, 639–645

Synthesis and mesomorphic properties of some esters of *trans*-4-*n*-alkoxycinnamic and *trans*-4-*n*-alkoxy-α-methylcinnamic acids exhibiting ferroelectric and antiferroelectric phases

by N. KASTHURAIAH, B. K. SADASHIVA*
Raman Research Institute, Bangalore-560 080, India

S. KRISHNAPRASAD and GEETHA G. NAIR
Centre for Liquid Crystal Research, Post Box 1329, Bangalore-560 013, India

(*Received 30 October 1997; accepted 3 November 1997*)

The synthesis and mesomorphic properties of several homologues of (*S*)-(+)-1-methylheptyl 4-[4 (*trans*-4-*n*-alkoxycinnamoyloxy)benzoyloxy]benzoates (series I) and (*S*)-(+)-1-methylheptyl 4-[4-(*trans*-4-*n*-alkoxy-α-methylcinnamoyloxy)benzoyloxy]benzoates (series II) are described. The influence of the α-methyl group on the different mesophases and the clearing temperatures has been evaluated. Many homologues of both the series show a ferroelectric chiral smectic C (SmC*) phase while the antiferroelectric smectic C phase (SmC_A^*) is exhibited by compounds of series I. The mesophases have been identified by optical polarizing microscopy, differential scanning calorimetry and miscibility studies. The spontaneous polarization, the helical pitch and the tilt angle of two of the compounds have also been measured.

1. Introduction

Since the discovery of the twist grain boundary phase in some phenyl propiolates by Goodby *et al.* [1] and the antiferroelectric chiral smectic C (SmC_A^*) phase by Chandani *et al.* [2], various compounds have been synthesized [3–9] which exhibit these phases. While the study of the twist grain boundary phase seems to be of academic interest, the SmC_A^* phase has been exploited for various device applications [10–12]. Generally, the SmC_A^* phase is accompanied by other sub-phases such as the SmC_α^* and the ferrielectric phases (SmC_γ^*). The appearance of one or more of these phases is influenced by small changes in the molecular structure of the chiral material under investigation. Goodby and co-workers [5, 13, 14] have shown that the appearance of the SmC_A^* phase is strongly dependent on the chirality of the molecules. For a clear understanding of the correlation between molecular structure and the appearance of the SmC_A^* phase a number of different types of compound have to be examined and many investigations are being carried out by various groups.

In this paper, we examine the appearance of the chiral smectic phases and compare the properties of two series of compounds, viz. (*S*)-(+)-1-methylheptyl 4-[4-(*trans*-4-*n*-alkoxycinnamoyloxy)benzoyloxy]benzoates, series I, and (*S*)-(+)-1-methylheptyl 4-[4-*trans*-4-*n*-alkoxy-α-methylcinnamoyloxy)benzoyloxy]benzoates, series II.

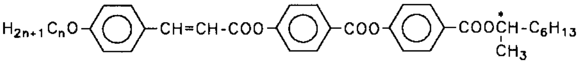

I

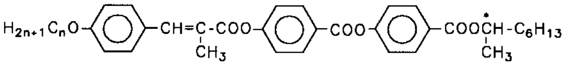

II

As can be seen, the two series of compounds differ from one another by a methyl group which is present in the α position of the cinnamic acid in series II. The effect of this lateral substituent on the mesophases will also be discussed.

The spontaneous polarization, helical pitch and optical tilt angle as functions of temperature have been measured for one homologue of each series; this probably represents the behaviour of the other homologues.

2. Synthesis and characterization of materials

The compounds of the two series, I and II, were prepared following the pathway shown in figure 1.

Benzyloxybenzoic acid (BBA) was prepared by treating ethyl 4-hydroxybenzoate with benzylchloride in the presence of anhydrous potassium carbonate in butan-2-one and hydrolysing the resulting ester with aqueous

---

*Author for correspondence.

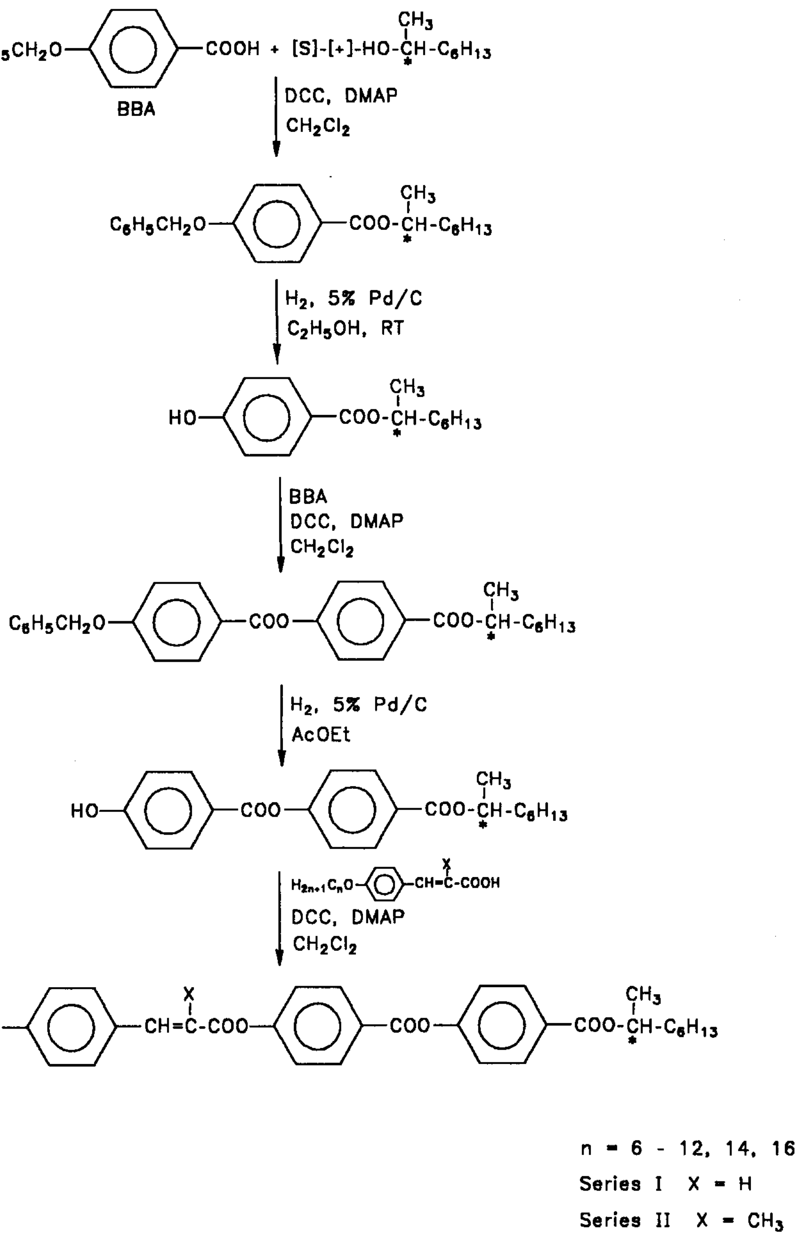

Figure 1. Synthetic pathway used for the preparation of the compounds of series I and II.

alkali. *trans*-4-*n*-Alkoxycinnamic acids [15] and *trans*-4-*n*-alkoxy-α-methylcinnamic acids [16] were prepared using procedures already described. The final compounds were prepared using the phenol 1-methylheptyl 4-(4-hydroxybenzoyloxy)benzoate and an appropriate *n*-alkoxycinnamic acid.

The intermediate and final compounds were purified by column chromatography on silica gel using chloroform as eluent. They were crystallized from suitable solvents. The purities of all these compounds were checked by thin layer chromatography (Merck Kieselgel 60F254 pre-coated plates) and by normal phase high performance liquid chromatography using μ porasil column (3·9 mm × 300 mm, Waters Associates Inc.) and 2% ethyl acetate in heptane as the eluent. The purities were found to be greater than 99%. The chemical structures of all the compounds were confirmed by using a combination of ^{1}H NMR spectroscopy (Bruker WP 80 SY spectrophotometer with tetramethylsilane as an internal standard), infrared spectroscopy (Shimadzu 1R435 spectrophotometer) and elemental analysis (Carlo-Erba 1106 analyser). Specific optical rotations were measured using dichloromethane as the solvent (Optical Activity AA 1000 polarimeter).

The detailed procedure for the synthesis and characterization of one of the compounds under study is given below.

(S)-(+)-1-Methylheptyl 4-[4-(trans-4-n-decyloxycinnamoyloxy)benzoyloxy]benzoate. A mixture of *trans*-4-*n*-decyloxycinnamic acid (142 mg, 0·46 mmol), (*S*)-(+)-1-methylheptyl 4-(4-hydroxybenzoyloxy)benzoate (180 mg, 0·46 mmol), *N*,*N*′-dicyclohexylcarbodiimide (DCC) (94 mg, 0·46 mmol) and anhydrous dichloromethane (10 ml) was stirred for two hours at room temperature. The *N*,*N*′-dicyclohexylurea formed was filtered off and the filtrate diluted with dichloromethane (25 ml). This solution was washed successively with water (2 × 30 ml), 5% aqueous acetic acid (3 × 50 ml), water (3 × 50 ml); it was then dried (Na_2SO_4). The residue obtained on removal of solvent was chromatographed on silica gel and eluted with chloroform. Removal of solvent from the eluate afforded a white solid material which was crystallized repeatedly from ethanol (267 mg, 87%), m.p. 86°C, $[\alpha]_D^{25} = 19{\cdot}27°$ ($5{\cdot}5\,\mathrm{mg\,ml^{-1}}$ in CH_2Cl_2), ν_{max}(nujol, $\mathrm{cm^{-1}}$) 1740, 1730, 1720 and 1605. ^{1}H NMR ($CDCl_3$, δ): 0·7–2·0 (35H, m, 3 × CH_3, 13 × CH_2), 4·1 (2H, t, $J = 6{\cdot}6$ Hz, $ArOCH_2$) 5·0–5·34 (1H, m, COOCH), 6·42 and 7·84 (AB q 2H, $J = 18{\cdot}6$ Hz, CH=CHCOO) 6·88 and 7·45 (4H, AB q, $J = 9{\cdot}0$ Hz, ArH), 7·32 and 8·16 (4H, AB q, $J = 9{\cdot}5$ Hz, ArH), 7·4 and 8·3 (4H, AB q, $J = 9{\cdot}0$ Hz, ArH). Elemental analysis: found, C 74·7, H 8·08%. $C_{41}H_{52}O_7$ requires C 75·0, H 7·92%.

3. Measurements

The phase assignments and transition temperatures were determined by thermal polarized light microscopy using a polarizing microscope (Leitz Laborlux 12 POL) equipped with a heating stage and a controller (Mettler FP52 and FP5, respectively), and also from thermograms recorded on a differential scanning calorimeter (Perkin-Elmer Model DSC-4 or Model DSC-7). These instruments were calibrated using pure indium as a standard.

The physical measurements were performed using samples sandwiched between ITO coated glass plates. Mylar spacers were used to define the thickness of the cell (typically ~10 μm for the polarization and tilt angle measurements and 100 μm for determination of the pitch). For spontaneous polarization (**P**) measurements, the triangular wave method [17, 18] was employed. To identify or confirm the presence of antiferroelectric and/or the ‘sub-phases’ a low frequency (0·97 Hz) probing field had to be used. However, the measurements as a function of temperature were carried out at a higher frequency (9·7 Hz) to avoid conductivity problems associated with low frequency, large magnitude fields. The tilt angle (θ) was measured by applying a near d.c. (0·1 Hz) switching field. The pitch values were determined by the optical diffraction method [19].

4. Results and discussion

The transition temperatures and associated enthalpies for compounds of the two series, I and II, are summarized in tables 1 and 2, respectively. As can be seen, the derivatives of *trans*-4-*n*-alkoxycinnamic acids show rich polymesomorphism. The mesophases were characterized by observing the textures in a planar arrangement of the samples as reported earlier [9], and by miscibility studies as discussed later in § 5. All the homologues exhibit a SmA phase and the clearing temperatures decrease with increasing length of the alkoxy chain; similarly the chiral smectic C phase is present in all the homologues, with compound **9** having the maximum thermal range of 58°C. The SmC_α^* phase precedes the other helical smectics in compounds **2**–**8** and the temperature range of this phase is rather narrow. Similarly the ferrielectric phase is exhibited by compounds **2**–**8**. This phase could be easily identified under the microscope as it fluctuates dynamically in homeotropic regions [7]. The antiferroelectric phase is also shown by the same seven compounds. The temperature range of this phase decreases with increase in length of the alkoxy chain. In homologous series I, compound **3** has the lowest melting point and the widest thermal range (44·5°C) of the antiferroelectric phase.

It can also be seen in table 1 that the enthalpies of transition between the antiferroelectric, ferrielectric, ferroelectric and SmC_α^* phases is extemely low; similar behaviour has been observed in a number of other homologous series [7, 8, 9]. A plot of the transition temperatures as a function of terminal alkyl chain length for series I is shown in figure 2. It is seen that there is a gradual decrease in the SmA → I transition temperatures while both SmC_α^* to SmA and SmC* to SmC_α^* transition points rise initially before levelling off.

The phase sequences, the accompanying transition temperatures and the enthalpies determined by thermal optical microscopy and differential scanning calorimetry for compounds of series II are summarized in table 2. One can see that compound **10** shows only a SmA phase, while the remaining homologues exhibit at least one other phase. Surprisingly, the antiferroelectric phase could not be observed in any of the compounds, although the ferrielectric and the SmC_α^* phases could still be retained. It is evident that the α methyl group has a dramatic effect on the stability of the SmC_A^* phase which is present in the unsubstituted compounds. In addition, the overall transition temperatures are lowered, as is to be expected [16]. Compounds **12** and **14** exhibit a monotropic phase (SmC_X^*) below the ferrielectric phase which is yet to be identified. By and large the melting

Table 1. Phase sequences, transition temperatures (°C) and (in italics) enthalpies (kJ mol^{-1}) for the compounds of series I. Cr = crystalline phase; SmC$^*_X$ = unidentified smectic phase; SmC$^*_A$ = antiferroelectric phase; SmC$^*_\gamma$ = ferrielectric phase; SmC* = ferroelectric phase; SmC$^*_\alpha$ = chiral smectic α phase; SmA = smectic A phase; I = isotropic phase.

Compound number	n	Cr		SmC$^*_A$		SmC$^*_\gamma$		SmC*		SmC$^*_\alpha$		SmA		I
1	6	•	107·2 *34·68*	—		—		•	118·0 *0·032*	—		•	178·4 *5·22*	•
2	7	•	92·5 *32·17*	•	117·0 *0·006*	•	119·0 *0·012*	•	131·7 *0·006*	•	133·0 *0·032*	•	172·0 *4·85*	•
3	8	•	79·5 *41·95*	•	124·0 *0·003*	•	126·0 *0·018*	•	140·0[a]	•	142·0 *0·119*	•	168·5 *4·45*	•
4	9	•	81·0 *26·0*	•	121·5 *0·014*	•	124·0 *0·025*	•	143·5 *0·013*	•	145·5 *0·224*	•	164·5 *4·1*	•
5	10	•	86·0 *34·83*	•	121·0 *0·007*	•	123·5 *0·044*	•	145·8[a]	•	148·5 *0·518*	•	161·0 *3·87*	•
6	11	•	87·0 *34·03*	•	109·0 *0·006*	•	112·0 *0·015*	•	145·0[a]	•	147·3 *0·596*	•	157·0 *2·94*	•
7	12	•	88·0 *35·49*	•	110·5 *0·013*	•	112·5 *0·009*	•	144·0[a]	•	145·8 *0·656*	•	154·5 *2·94*	•
8	14	•	85·5 *46·63*	•	93·5 *0·01*	•	96·0 *0·016*	•	142·0[a]	•	143·7 *0·704*	•	151·0 *2·42*	•
9	16	•	83·0 *32·93*	—		—		•	141·0 *1·25*	—		•	147·0 *1·77*	•

[a] Enthalpy could not be determined.

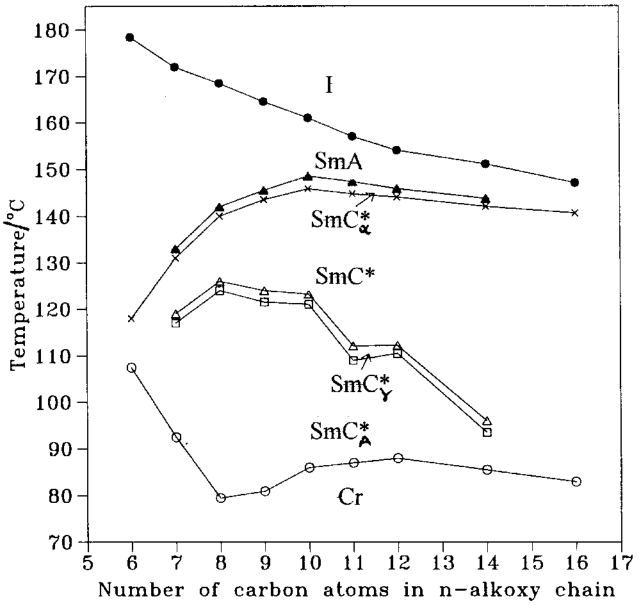

Figure 2. Plot of transition temperatures as a function of n-alkyl chain length for series I.

points are relatively lower in comparison with those obtained for compounds of series I. A plot of the transition temperatures versus the number of carbon atoms in the terminal chain is shown in figure 3. The trends of the different curves are similar to those observed for series I, except that the slopes are different.

5. Mixture studies

As already mentioned, the compounds of series I show rich polymesomorphism. In order to identify and confirm the assignment of the various smectic mesophases an isobaric binary phase diagram was constructed using mixtures of compound **3** and the standard material 4-(1-methylheptyloxycarbonyl)phenyl 4′-n-octyloxybiphenyl 4-carboxylate (MHPOBC). The mixtures were made as weight/weight ratios and mixed thoroughly in their isotropic states. The transition temperatures and the identities of the different mesophases were determined by using a combination of optical microscopy and differential scanning calorimetry. The isobaric binary phase diagram obtained is shown in figure 4. It is clear from this diagram that there is continuous miscibility of the SmA, SmC$^*_\alpha$, SmC*, SmC$^*_\gamma$ and SmC$^*_A$ phases over the entire composition range, confirming the optical observations. Also, since the chiral phases exist over the entire composition range, the helical twist sense of the two compounds is the same.

6. Electro-optical studies

Figures 5 and 6 show the current response to an applied triangular wave in the different mesophases of compounds **5** and **12**, respectively. The patterns of these oscilloscope traces show clear signatures of the underlying switching mechanisms in each of the phases and are in agreement with those reported in the literature.

Table 2. Phase sequences, transition temperatures (°C) and (in italics) enthalpies (kJ mol^{-1}) for the compounds of series II. Cr = crystalline phase; SmC$_x^*$ = unidentified smectic phase; SmC$_A^*$ = antiferroelectric phase; SmC$_\gamma^*$ = ferrielectric phase; SmC* = ferroelectric phase; SmC$_\alpha^*$ = chiral smectic α phase; SmA = smectic A phase; I = isotropic phase.

Compound number	n	Cr		SmC$_x^*$		SmC$_\gamma^*$		SmC*		SmC$_\alpha^*$		SmA		I
10	8	•	58·5 *32·93*	—		—		—		—		•	119·5 *5·58*	•
11	9	•	57·5 *43·36*	—		—		(•	52·5) *0·003*	•	59·6 *0·085*	•	115·5 *4·85*	•
12	10	•	62·5 *44·47*	(•	59·5) *0·026*	•	69·5 *0·01*	—		•	73·5 *0·02*	•	114·0 *5·89*	•
13	11	•	60·7 *33·0*	—		—		•	84·2 *0·005*	•	88·0 *0·008*	•	113·7 *5·4*	•
14	12	•	57·0 *52·76*	(•	40·0) *0·027*	•	62·1 *0·279*	•	90·6 *0·016*	•	93·0 *0·02*	•	113·0 *5·44*	•
15	14	•	64·2 *41·23*					•	94·0 *0·152*			•	110·0 *4·28*	•

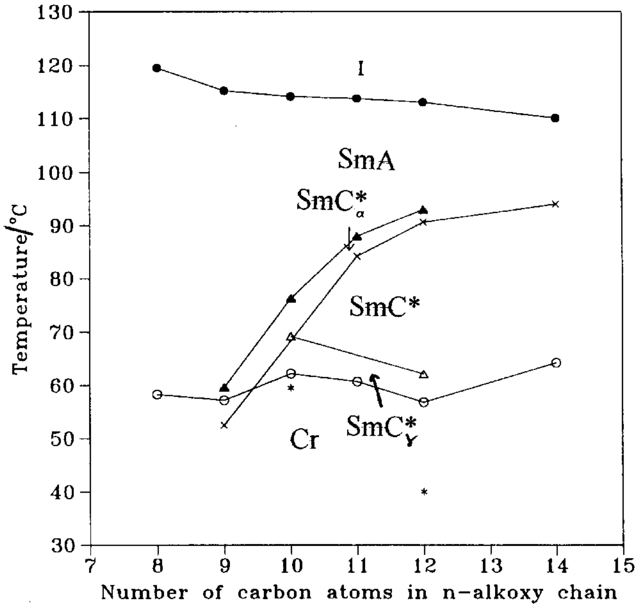

Figure 3. Plot of transition temperatures as a function of *n*-alkyl chain length for series II.

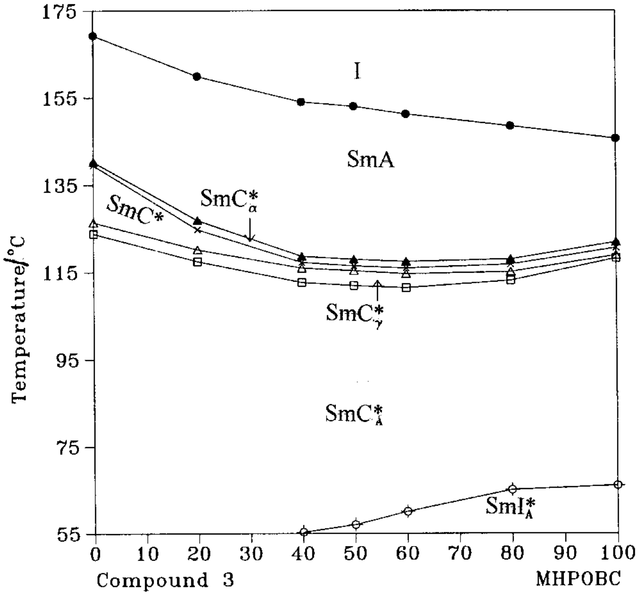

Figure 4. Miscibility phase diagram of binary mixtures of compound **3** and the standard material MHPOBC.

But it must be remarked that the strength of the additional peaks in the SmC$_\alpha^*$ and SmC$_\gamma^*$ phases (compare the panels in the two figures) varies from one material to another, a feature observed in our earlier study also [9]. Perhaps it is controlled by the nature of the phase transition at a lower temperature. For example, in the case of compound **5**, which shows weaker additional peaks, the SmC$_\alpha^*$ to SmC$_\gamma^*$ transformation is through the C* phase. In contrast in compound **12**, having very strong additional peaks, the transition is direct. These features are reflected in the associated transition enthalpies. Of course more studies are needed to see whether this is generally applicable to all systems.

The temperature dependence of polarization (**P**) for compound **5** is shown in figure 7. The smooth variation through the different phases shows that the applied field was high enough to transform the structure in the SmC$_A^*$ to SmC$_\gamma^*$ phase to the ferroelectric state. In other words the applied field was greater than the helix unwinding field. Comparing the saturated value of **P** obtained for structurally similar compounds, it is observed that compound **5** shows a slightly higher **P** than a compound [20] which has no bridging group between the first and second phenyl rings (as seen from the non-chiral chain side). The presence of a transverse dipole moment (C=O) in this position for compound **5**

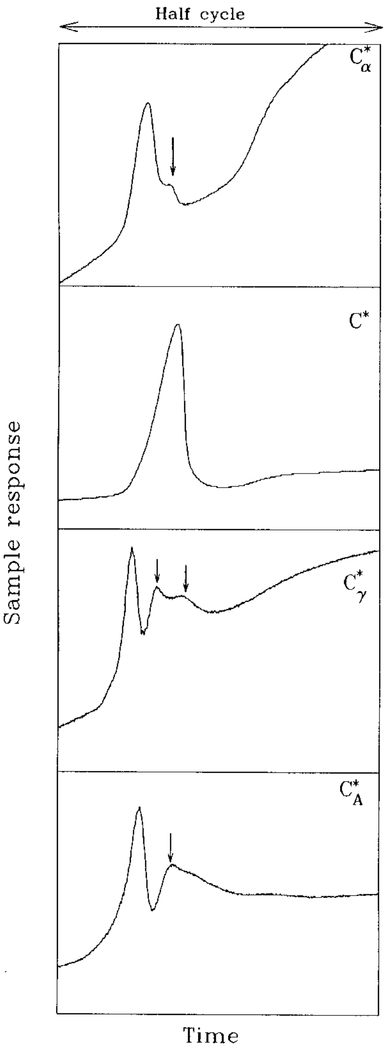

Figure 5. Raw oscilloscope traces in the smectic SmC_α^*, SmC*, SmC_γ^*, and SmC_A^* phases of compound **5**.

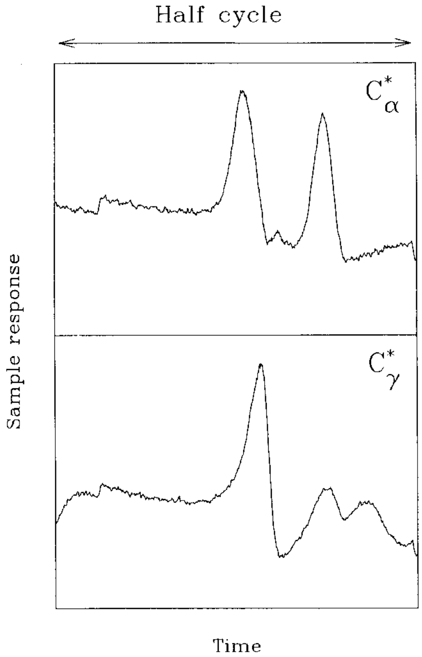

Figure 6. Raw oscilloscope traces in the smectic SmC_α^*, and SmC_γ^* phases of compound **12**.

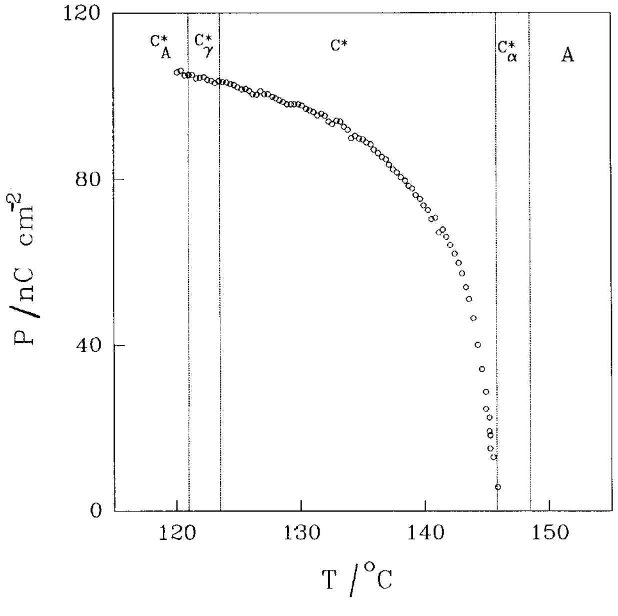

Figure 7. Thermal variation of polarization (**P**) for compound **5**.

is perhaps the cause. However, the introduction of the C=O dipole between the second and third phenyl rings seems to affect adversely the magnitude of **P**. For example, compare the value for compound **5** with that for compound 9, chbp 16 (*R*) reported by Tuffin *et al.* [21]; a similar feature was reported by Robinson *et al.* [20]. The reason could be that due to packing considerations the C=O dipole between the second and third phenyl ring and the one attached to the chiral chain are forced to point in opposite directions, thus reducing the effective dipole moment.

Plots of optical tilt angle and helical pitch as functions of reduced temperature T_c-T (where T_c is the SmC_α^*–SmC* transition temperature) for compound **5** are shown in figures 8 and 9, respectively. The tilt angle is seen to have appreciable temperature dependence, a feature which is in contradiction to that observed in another compound [9] having the same transition. As remarked above, the additional peaks in the current response oscilloscope traces taken in the SmC_α^* phase are much weaker for compound **5** than the one obtained for the compound used in the earlier study [9]. Perhaps the SmC_α^*–SmC* transition is much weaker in the present case. This is similar to the observation that the tilt angle variation in the SmC* phase depends on whether the transition to the high temperature phase is

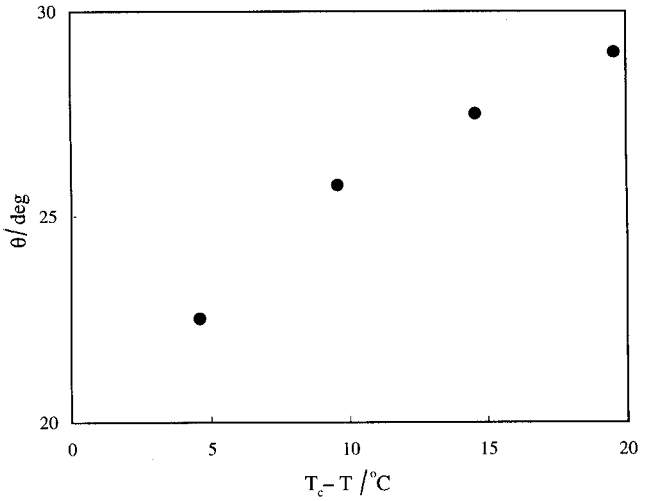

Figure 8. Plot of reduced temperature ($T_C - T$) versus optical tilt angle for compound **5**.

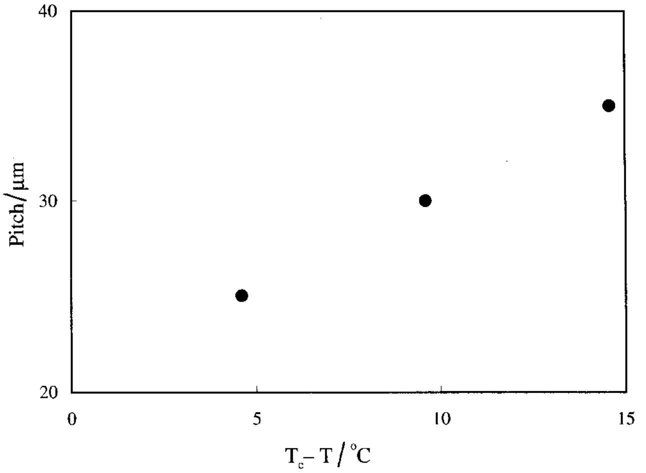

Figure 9. Plot of reduced temperature ($T_C - T$) versus helical pitch for compound **5**.

first or second order. In the temperature dependence of the helical pitch also (see figure 9), one observes a similar contrast in the behaviour between compound **5** and the one used by us in the earlier work. However, it is not clear whether the pitch variation in the SmC* phase would be influenced by the nature of the SmC^*_α–SmC* transitions.

7. Conclusions

Two series of chiral *trans*-4-*n*-alkoxycinnamic acid derivatives have been prepared which differ from one another by an α-methyl substituent. Though this methyl substituent does not greatly enhance the lateral dimensions of the molecule, it has a significant effect not only on the sequence of the chiral mesophases but also on the transition temperatures. Importantly, the antiferroelectric SmC^*_A phase seen in the unsubstituted compounds becomes completely eliminated in the α-methyl substituted compounds. Also, in one of these homologues, there is a direct transition from the SmC^*_α to the SmC^*_γ phase which is a rather rare occurrence.

The authors would like to thank Mr K. Subramanya for recording the various spectra and for carrying out elemental analyses. They are grateful to Dr H. T. Nguyen and Dr J. C. Rouillon of Centre de Recherche Paul Pascal, Bordeaux, France for the differential scanning calorimetric data on some of the compounds.

References

[1] Goodby, J. W., Waugh, J. W., Stein, M. A., Chin, S. M., Pindak, E., and Patel, J. S., 1989, *Nature*, **337**, 449.
[2] Chandani, A. D. L., Gorecka, E., Ouchi, Y., Takezoe, H., and Fukuda, A., 1989, *Jpn. J. appl. Phys.*, **28**, L1265.
[3] Goodby, J. W., Waugh, J. W., Stein, M. A., Chin, S. M., Pindak, R., and Patel, J. S., 1989, *J. Am. chem. Soc.*, **111**, 8119.
[4] Bouchta, A., Nguyen, H. T., Achard, M. F., Hardouin, F., Destrade, C., Twieg, R. J., Maaroufi, A., and Isaert, N., 1992, *Liq. Cryst.*, **12**, 575.
[5] Goodby, J. W., Patel, J. S., and Chin, E., 1992, *J. mater. Chem.*, **2**, 197.
[6] Inui, S., Suzuki, T., Iimura, N., Iwane, H., and Nohira, H., 1994, *Mol. Cryst. liq. Cryst.*, **239**, 1.
[7] Nguyen, H. T., Rouillon, J. C., Cluzeau, P., Sigaud, G., Destrade, C., and Isaert, N., 1994, *Liq. Cryst.*, **17**, 571.
[8] Faye, V., Rouillon, J. C., Destrade, C., and Nguyen, H. T., 1995, *Liq. Cryst.*, **19**, 47.
[9] Kasthuraiah, N., Sadashiva, B. K., Krishnaprasad, S., and Nair, G. G., 1996, *J. mater. Chem.*, **6**, 1619.
[10] Yamamoto, N., Yamada, Y., Koshobu, Y., Mori, K., Nakamda, K., Orihara, H., Ishibashi, Y., Suzuki, Y., and Kawamura, I., 1992, *Jpn. J. appl. Phys.*, **31**, 3186.
[11] Noriyama, T., Kajita, J., Takanishi, Y., Ishikawa, K., Takezoe, H., and Fukuda, A., 1993, *Jpn. J. appl. Phys.*, **32**, 589.
[12] Orama, T., Masuda, T., Hamada, S., Takahashi, S., Kurita, S., Kawamura, I., and Hagiwara, T., 1993, *Jpn. J. appl. Phys.*, **32**, L668.
[13] Nishiyama, I., and Goodby, J. W., 1993, *J. mater. Chem.*, **3**, 149.
[14] Goodby, J. W., Nishiyama, I., Slaney, A. J., Booth, C. J., and Toyne, K. J., 1993, *Liq. Cryst.*, **14**, 37.
[15] Gray, G. W., and Jones, B., 1954, *J. chem. Soc.*, 1467.
[16] Sadashiva, B. K., 1976, *Mol. Cryst. liq. Cryst.*, **35**, 205.
[17] Miyasato, K., Abe, S. Takezoe, H., Fukuda, A., and Kuze, E., 1983, *Jpn. J. appl. Phys.*, **22**, L661.
[18] Krishnaprasad, S., Nair, G. G., and Chandrasekhar, S., 1995, *J. mater. Chem.*, **5**, 2253.
[19] Krishnaprasad, S., and Nair, G. G., 1991, *Mol. Cryst. liq. Cryst.*, **202**, 91.
[20] Robinson, W. K., Miller, R. J., Gleeson, H. F., Hird, M., Seed, A. J., and Styring, P., 1996, *Ferroelectrics*, **178**, 237.
[21] Tuffin, R. P., Goodby, J. W., Bennemann, D., Heppke, G., Lozsch, D., and Scherowsky, G., 1995, *Mol. Cryst. liq. Cryst.*, **260**, 51.